Decoupling crossover in asymmetric broadside coupled split-ring resonators at terahertz frequencies

Keiser, G. R.; Strikwerda, Andrew; Fan, K.; Young, V.; Zhang, X.; Averitt, R. D.

Published in:
Physical Review B Condensed Matter

Link to article, DOI:
10.1103/PhysRevB.88.024101

Publication date:
2013

Document Version
Publisher's PDF, also known as Version of record

Decoupling crossover in asymmetric broadside coupled split-ring resonators at terahertz frequencies

G. R. Keiser,[1,*] A. C. Strikwerda,[1,3] K. Fan,[2] V. Young,[1] X. Zhang,[2] and R. D. Averitt[1]
[1]*Boston University, Department of Physics, Boston, Massachusetts 02215, USA*
[2]*Boston University, Department of Mechanical Engineering, Boston, Massachusetts 02215, USA*
[3]*Technical University of Denmark, DTU Fotonik—Department of Photonics Engineering, Kgs. Lyngby, DK-2800, Denmark*
(Received 6 February 2013; revised manuscript received 17 June 2013; published 3 July 2013)

We investigate the electromagnetic response of asymmetric broadside coupled split-ring resonators (ABC-SRRs) as a function of the relative in-plane displacement between the two component SRRs. The asymmetry is defined as the difference in the capacitive gap widths (Δg) between the two resonators comprising a coupled unit. We characterize the response of ABC-SRRs both numerically and experimentally via terahertz time-domain spectroscopy. As with symmetric BC-SRRs ($\Delta g = 0$ μm), a large redshift in the LC resonance is observed with increasing displacement, resulting from changes in the capacitive and inductive coupling. However, for ABC-SRRs, in-plane shifting between the two resonators by more than 0.375 L_o (L_o = SRR sidelength) results in a transition to a response with two resonant modes, associated with decoupling in the ABC-SRRs. For increasing Δg, the decoupling transition begins at the same relative shift (0.375 L_o), though with an increase in the oscillator strength of the new mode. This strongly contrasts with symmetric BC-SRRs, which present only one resonance for shifts up to 0.75 L_o. Since all BC-SRRs are effectively asymmetric when placed on a substrate, an understanding of ABC-SRR behavior is essential for a complete understanding of BC-SRR based metamaterials.

DOI: 10.1103/PhysRevB.88.024101 PACS number(s): 81.05.Xj, 78.67.Pt

Metamaterials (MMs) present a vast array of exciting possibilities for optical materials engineering, allowing for the design and fabrication of materials where the electric permittivity, magnetic permeability, and impedance can be specified with ever-increasing precision. Split-ring resonators (SRRs), first proposed by John Pendry,[1] are ubiquitous in MM designs, appearing in negative index materials,[2,3] electromagnetic cloaks,[4] memory MMs,[5] thermal detectors,[6] and perfect absorbers[7,8] to name just a few representative examples. As the field has progressed, geometrical variants on the basic SRR have appeared in the literature.[9–11] The push for tunable and controllable MM devices[12] has ignited interest in SRR variants where manipulation of near field coupling can be used to alter a MM response.[13] Manipulation of coupled MM structures has born much fruit in recent years, especially in the areas of tunable[14] and nonlinear MMs.[15] In particular, broadside coupled SRRs (BC-SRRs)[16] have attracted considerable attention due to their high structural tunability[13,17] and ability to eliminate parasitic bianisotropic effects at the unit cell level.[18]

To date, the majority of research on the transmission characteristics and tunability of BC-SRRs has focused on designs where both rings have identical resonance frequencies.[17,19] Only one exception, a small subsection of Ref. 20, is known to the authors. There are, however, several ways in which BC resonators become effectively asymmetric, meaning that the two resonators have different resonant frequencies. For example, the presence of a substrate will break symmetry and induce bianisotropy into any MM design,[21] including planar BC-SRRs. It is also possible to create asymmetric BC-SRRs (ABC-SRRs) by varying the relative geometrical parameters (and hence capacitance and inductance) of the SRRs that comprise the BC-SRR unit. Given the multiple ways in which asymmetry can be introduced into coupled resonators (either on purpose or spuriously), systematic research into the electromagnetic properties of ABC-SRRs is vital to gain a more complete understanding of MMs.

We expand on the results of previous work on symmetric BC-SRRs[17,19,22] by investigating how an in-plane, lateral shift (see Fig. 1) between the two elements composing an ABC-SRR affects the response of the MM as a whole. This is accomplished by fabricating stand-alone ABC-SRR structures in polyimide where the asymmetry is defined by the difference in the gap widths (Δg) in the two resonators. For a given Δg, the lateral shift is varied, and the resulting electromagnetic response experimentally measured using terahertz time-domain spectroscopy (THz-TDS). Our electrically active MMs (i.e., resonant under excitation by the terahertz electric field) exhibit a large redshift in the fundamental mode as a function of increasing lateral shift between the SRRs. This effect is due to the shift-induced change in near-field coupling between the SRRs comprising the ABC-SRRs.[17,23] Of particular significance, a second resonance appears for shifts greater than 0.375 L_o, where L_o is the side length of the component SRRs (Fig. 1). This dramatic change of behavior arises as the ABC-SRR transitions to a decoupled state for large shift values, defined as a state where the component SRRs respond to incident radiation as separate, individual resonators. Full-wave electromagnetic simulations confirm this explanation. This behavior is in stark contrast to the behavior of a symmetric BC-SRR, which shows only one coupled mode for all shift values up to 0.75 L_o.[17] We conclude by providing intuitive explanations for this disparate behavior, consistent with the conceptual models published in previous work.

The design of the ABC-SRR structures is outlined in Fig. 1. The unit cell of the MM is composed of two square SRRs separated by a 5-μm polyimide substrate [$\varepsilon_r = 2.88$ loss-tangent $\tan(\delta) = 0.0313$]. The rings are rotated 180° relative to each other, producing a BC configuration (Fig. 1). Both

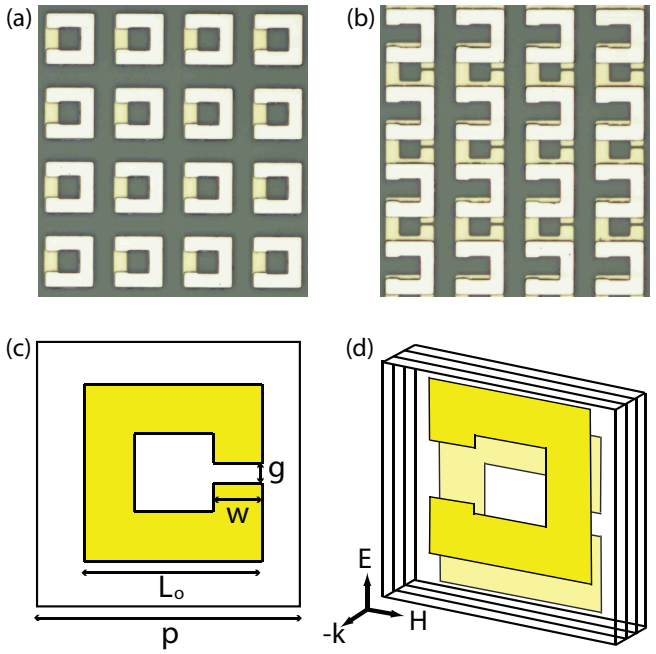

FIG. 1. (Color online) (a) Photograph of unshifted ABC-SRR array. The front gap is $g = 16$ μm, while the back gap is $g_{\text{back}} = 2$ μm. (b) Photograph of shifted ABC-SRR array. The dimensions are the same as in (a). (c) Top-down schematic of ABC-SRR unit cell, showing the top ring and relevant dimensions. (d) Perspective view of ABC-SRR unit cell showing the direction of lateral shifting and the polarization and direction of the terahertz signal used to excite the MMs.

rings are then covered with a 5-μm polyimide superstrate. The dimensions of an individual ring are shown in Fig. 1(c). The unit-cell periodicity is $P = 60$ μm, metallization side-length $L_o = 40$ μm, metallization width $w = 11$ μm, front gap width $g = 2$ μm, and the back gap width varies from 4 μm to 16 μm in 4-μm steps. The lateral shift (L_{shift}) between the two rings [Fig. 1(d)] varies from 0 μm to 25 μm in 5-μm steps. The dimensions are such that a 30-μm shift is equal to a shift of half a unit cell. For purposes of comparison, single-layer SRR samples with varying gap widths were fabricated along with the ABC-SRR structures. All samples were fabricated using conventional photolithography, as described in detail in Ref. 17.

Following fabrication, the MMs were characterized using THz-TDS. The radiation was normally incident and oriented so the electric field is parallel to the sides of SRRs with the capacitive gaps. This ensures that we are exciting the structures via the electric field and not the magnetic field since the incident magnetic field does not thread the SRRs [Fig. 1(d)].

The transmission as a function of frequency for structures with 0-μm lateral shift and 25-μm lateral shift are shown in Figs. 2(b) and 2(c), respectively. For each lateral shift, the data is shown for $\Delta g = 2$, 6, 10, and 14 μm. For the unshifted case [Fig. 2(b)], a single resonance is observed, blueshifted from the uncoupled resonances of the individual component SRRs presented in Fig. 2(a). For easy comparison, the transmission spectrum of a single SRR with $g = 2$ μm is included in all plots of Fig. 2 (dashed curves). This blueshifted resonance corresponds to the expected electrical resonance of

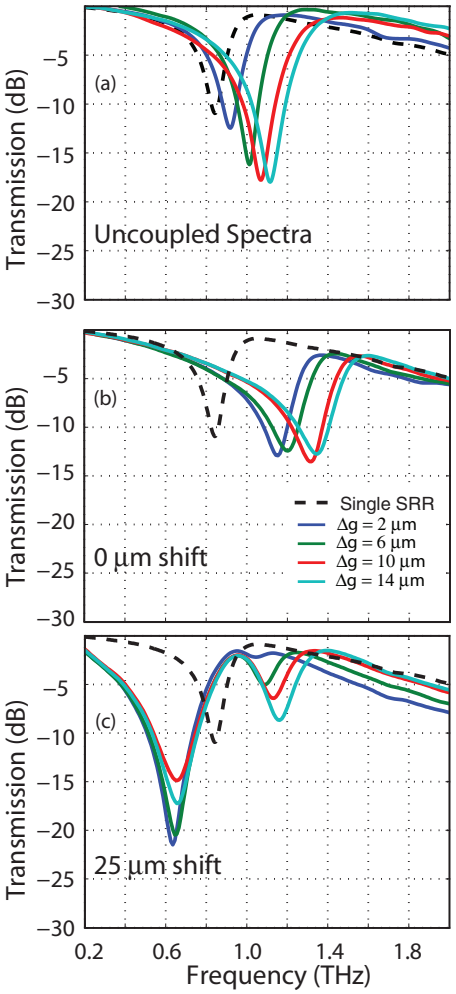

FIG. 2. (Color online) (a) Experimental transmission spectra for single-layer SRRs for varying capacitative gap widths. (b) Experimental transmission spectra for ABC-SRRs with varying gap differences. In this unshifted case, only the fundamental electrical resonance of the ABC-SRR is excited. For comparison, the black dashed curve shows the experimental transmission spectrum for a single, uncoupled SRR with $g = 2$ μm. (c) Experimental transmission curves for the corresponding 25-μm shifted ABC-SRRs. Here, the electrical resonance has redshifted, consistent with Ref. 17. However, a new mode appears at higher frequencies and is strongly dependent on the asymmetry between the SRRs. For comparison, the black dashed curve shows the experimental transmission spectrum for a single, uncoupled SRR with $g = 2$ μm. Plots are scaled in dB for clarity, as some resonances are very wide when plotted on a linear scale.

a BC-SRR. This mode involves circular currents distributions in the component SRRs, circulating clockwise in one SRR and counterclockwise in the other SRR. This resonance behavior is described in detail in Ref. 17.

In contrast, in the 25-μm shifted case [Fig. 2(c)], two modes are excited. A strong electrical resonance now appears at frequencies lower than the bare single-element SRR resonance frequencies [i.e., see Fig. 2(a)], and the second resonance appears at frequencies higher than the uncoupled resonance frequencies. The oscillator strength of this second resonance depends on the asymmetry between the SRRs,

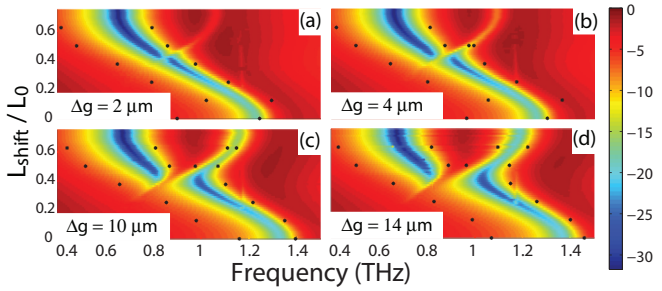

FIG. 3. (Color online) Simulation results showing transmission (in dB) curves vs shift for (a) 2-μm, (b) 4-μm, (c) 10-μm, and (d) 14-μm gap differences. Shift distances are normalized to the side length of the SRRs, L_o. Asterisks denote the experimental -7 dB points and are included to show correspondence of simulation with experiment.

growing larger with increasing Δg. One possibility is that this second mode is the ABC-SRR's other magnetic mode, excited through the bianisotropy inherent in the asymmetric resonator design. Such a mode consists of circular currents in the SRRs that now circulate in the same direction in both rings.[17] However, this is not the case. If it were, one would expect a resonance of approximately equal strength to appear at lower frequencies for shifts smaller than $L_{\text{shift}}/L_o = 0.375$ as well.[19] In the following, it is demonstrated that the appearance of the second mode arises as the individual SRRs comprising the ABC-SRR unit cell start responding to incident radiation separately, as individual, uncoupled resonators. Summarizing the results of Fig. 2, for unshifted resonators [Fig. 2(b)], varying Δg causes no significant effects on the electromagnetic response. In contrast, for shifted resonators [Fig. 2(c), $L_{\text{shift}} > 0.375\ L_o$], a new mode appears for $\Delta g > 0$ μm with a magnitude that increases with the magnitude of Δg.

In order to shed light on the phenomena involved, the electromagnetic response of the ABC-SRRs was modeled using the frequency solver in CST Microwave Studio. The simulated transmission vs L_{shift} for multiple values of Δg are presented and compared with the experiment in Fig. 3. As the figure demonstrates, two resonances are excited for shift values greater than $0.375\ L_o$, and the strength of this resonance increases as Δg is increased.

There are several common approaches used to model the behavior of a BC-SRR or other coupled MM systems. Coupled mode theory[23] is perhaps one of the most familiar and accessible approaches. In addition, a mode hybridization model for coupled plasmonic systems and MMs (Ref. 24) provides illuminating analogies to systems in other fields of study, including chemistry.[25] Ekmekci *et al.*[17] proposed a consistent, third coupling model for a BC-SRR based on mutual capacitance and inductance that has provided an intuitive and direct approach for the study of shifted BC-SRR systems. Below, we follow this third approach.

Consider the trend of the single mode for $L_{\text{shift}} < 0.375\ L_o$. This primary mode of the structure moves to lower frequencies as L_{shift} is increased. This is due to the shift-induced change in mutual capacitance and inductance between the two SRRs. For $L_{\text{shift}} = 0$ μm, the mode is blueshifted from the bare resonance of a lone SRR due to capacitive and inductive coupling between the rings. The mutual inductance starts out negative and increases with shift. The mutual capacitance also increases with the shift, since the positive charge distribution of one SRR is moved closer to the negative charge distribution on the other SRR. Thus, as the SRRs are shifted laterally, the total capacitance and inductance will increase, decreasing the resonance frequency since $\omega_o \sim 1/\sqrt{(LC)}$. The resulting effect on this mode is to redshift until it undergoes an avoided crossing with the magnetic resonance of the structure (not excited in the experimental configuration at normal incidence) at $0.375\ L_o$.

For further shifts, two resonant modes couple to the terahertz electric field. The lower frequency resonance redshifts until $L_{\text{shift}} = 0.75\ L_o$. The higher frequency resonance experiences a slight blueshift over the same range. For shifts greater than $0.75\ L_o$, the SRRs begin to overlap with the SRRs from neighboring unit cells, resulting in the reverse process with a corresponding blueshift for the low frequency mode and a corresponding redshift for the high frequency mode back to the resonance positions for $L_{\text{shift}} = 0.375\ L_o$. For even larger shifts, the ABC-SRR transitions back to single mode behavior, with the mode blueshifting back to the resonance position at $L_{\text{shift}}/L_o = 0$.

The appearance of the second high frequency mode for $L_{\text{shift}}/L_o > 0.375$ is present only for large shift values and has an oscillator strength strongly dependent on the asymmetry between the SRRs [Figs. 2(b) and 3], signaling the onset of new behavior not observed in previous work focusing solely on symmetric BC-SRRs.

Further insight into the physical mechanism behind the appearance of this higher frequency resonance becomes apparent by considering the response of an ABC-SRR structure with a larger unit cell. In this case, we have doubled the size in the y direction to create a rectangular unit cell with $P_y = 2P_x = 120$ μm while leaving all other SRR dimensions the same. This change will increase the space between each ABC-SRR and its nearest neighbor in the direction of L_{shift}. Figure 4(a) shows the simulated transmission response of such a structure. Since the SRRs can now be shifted without overlapping with a resonator from another unit cell, we can investigate the continuing trend in the response for $L_{\text{shift}} > 0.75\ L_o$ (30 μm). Figure 4(a) shows that the two resonances which appear at $L_{\text{shift}} = 0.375\ L_o$ (15 μm) trend to the uncoupled, bare resonance frequencies of the individual SRRs. Figure 4(b) shows the magnitude of the on-resonance surface current densities in both SRRs for $L_{\text{shift}} = 0$ μm. The spatial current distribution in the SRRs in Fig. 4(b) is characteristic of the lowest order resonant mode of a BC-SRR, indicating that the two SRRs are responding to the incident electrical excitation as one strongly coupled resonator in this regime.

When Fig. 4(b) is compared to Figs. 4(c) and 4(d), significantly different behavior is observed. Figures 4(c) and 4(d) show the surface current densities in both SRRs for $L_{\text{shift}} = 1.5\ L_o$ at $f = 0.8$ THz and $f = 1.1$ THz, respectively. It is apparent that the 0.8 THz resonance is driven by currents excited predominately in the small gap SRR, while the 1.1 THz resonance is driven by currents excited predominately in the large gap SRR. Thus, when L_{shift} is increased beyond $0.375\ L_o$, the system trends to a state where the individual SRRs respond to incident radiation as separate elements. Thus, there are two

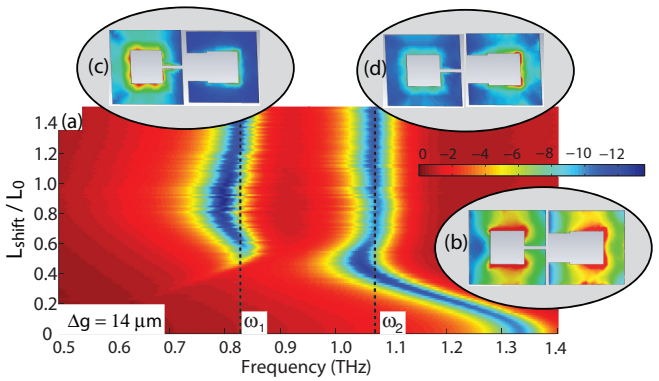

FIG. 4. (Color online) (a) Simulation results showing transmission curves (in dB) vs lateral shift for an ABC-SRR with a 14-μm gap difference in a rectangular unit cell lattice ($P_y = 2\ P_x = 120\ \mu$m). All other dimensions are the same as in the previous structures. The dotted lines at ω_1 and ω_2 correspond to the uncoupled resonance frequencies of the smaller gap SRR and the larger gap SRR, respectively. Shift distances are normalized to the side length of the SRR, L_o. In this large unit cell lattice the SRRs can be shifted far enough apart to completely decouple from each other and from SRRs in the nearest neighbor cells. As the SRRs are shifted, the two resonances trend to the uncoupled resonance frequencies. (b) Resonance surface current density in arbitrary units in both SRRs for $L_{\text{shift}} = 0\ L_o$, showing that at the 1.3 THz resonance the SRRs are equally excited and acting as one coupled resonator. (c) Resonance surface current density in arbitrary units in both SRRs for $L_{\text{shift}} = 1.5\ L_o$ and $f = 0.8$ THz, showing that the response is dominated by currents in the small gap SRR. (d) Resonance surface current density in arbitrary units in both SRRs for $L_{\text{shift}} = 1.5\ L_o$ and $f = 1.1$ THz, showing that the response is dominated by currents in the large gap SRR. Thus, for large shifts, the SRRs are excited separately, as uncoupled resonators.

separate resonant modes, with frequencies determined by the subgeometry of the individual SRRs and not their relative lateral displacement. The SRRs are now effectively individual, decoupled resonators for $L_{\text{shift}}/L_o > 0.375$.

Note that the spatial current density in the SRRs shown in Fig. 4(b) is non-uniform. The regions of lower current density in the SRR might appear, upon initial inspection, to be nodes in the current density distribution. This would indicate higher order SRR modes being involved in the coupled response since this behavior is not expected in the two lowest frequency resonances of a BC-SRR. However, the direction of the current in the SRRs, while not included in Fig. 4 for the purposes of clarity, remains the same across the entire surface of each SRR, indicating that the regions of low current density are not true nodes in the SRR current. Since the SRR current flows in the same direction at all points around each SRR, only the lowest order LC modes of the individual SRRs are involved in the coupled response, as one would expect.

Many aspects of the shifted ABC-SRR's two-mode response become intuitive when the conceptual models of Refs. 17 and 19 are applied. The capacitive coupling depends on the charge distribution in the individual SRR gaps and the SRR's lateral displacement.[17] As the gap in a ring is made larger, the charge buildup in the SRR gap will decrease in magnitude. This effectively lowers the capacitive coupling between the SRRs, making the SRRs more prone to decoupled behavior for larger Δg. This explains the Δg dependence for the strength of the higher frequency resonance.

Indeed, this behavior is entirely consistent with a coupled oscillator model for the ABC-SRR. Increasing L_{shift} will decrease the electromagnetic coupling between the resonators. The coupling is also lowered by increasing Δg, as discussed above. The simplest analogy comes in the form of two block/spring systems with spring constants, k_1 and k_2 coupled via a third spring with spring constant κ. For $\kappa \ll k_1, k_2$ (low coupling between the oscillators), the two systems will tend to oscillate separately at their own uncoupled resonance frequencies. Thus, for sufficiently large Δg, the spring system will oscillate at two easily distinguishable uncoupled modes. In this view, while this behavior has not been seen before in BC-SRRs, it is no surprise the resonators tend to decouple with increasing shift, and that two resonances appear for sufficiently high Δg.

The onset point of the crossover can also be understood conceptually. As the two SRRs are shifted laterally, the magnetic and electric coupling parameters defined in Ref. 19 both become zero for a shift value corresponding to $L_{\text{shift}} = 0.375\ L_o$ in this work. It is at this point of minimum interaction where the ABC-SRRs are able to transition from coupled to decoupled behavior, and the two-mode state appears. As the two SRRs are shifted beyond $L_{\text{shift}} = 0.375\ L_o$, the coupling parameters briefly increase before asymptotically approaching 0 as the ABC-SRRs are shifted infinitely far apart. This increase in coupling gives rise to a transition region between the one- and two-mode states. In this region, which is clearly visible in Figs. 3 and 4(a), two resonances appear but are still shifted slightly from the bare SRR resonance frequencies.

Finally, while this decoupling transition was not observed in the previous studies on symmetric BC-SRRs,[17,19] the results presented in this paper are consistent with previous work. For the symmetric ($\Delta g = 0\ \mu$m) BC-SRR structures considered previously, decoupled behavior is not observed for two reasons. First, the two uncoupled resonators are degenerate, allowing for only one electric mode at all shift values. Additionally, as the previous work focused on square unit cells with small periodicity, it was impossible to shift the BC-SRRs out of the transition region discussed above. The net effect is a resonant response with one mode that exhibits coupled behavior for all accessible values of L_{shift}.

In summary, we investigated the response of asymmetric BC-SRRs (ABC-SRRs) under lateral shift using THz-TDS and numerical simulations. We observe a transition from a one-resonance state to a two-resonance state for shift values larger than $L_{\text{shift}}/L_{\text{o}} = 0.375$, where L_o is the side length of an SRR. For lateral shifts lower than this value, the ABC-SRRs act as one coupled resonant element. Above this value, the component SRRs respond to incident radiation as separate, uncoupled resonators, as evidenced by the simulated on-resonance surface current densities. This behavior is consistent with the previously published results for symmetric BC-SRR structures and can be explained using similar conceptual models. As substrate-induced bianisotropy, fabrication error, and other effects can conspire to make symmetric BC-SRRs effectively asymmetric, these results provide a description of ABC-SRR behavior essential for complete understanding of BC-SRR based MMs.

The authors acknowledge support from DTRA C&B Technologies Directorate administered through a subcontract from ARL, from NSF under Contract No. ECCS 0802036, and AFOSR under Contract No. FA9550-09-1-0708. The authors would also like to thank the Photonics Center at Boston University for technical support throughout this project.

*grkeiser@physics.bu.edu

[1] J. B. Pendry, A. J. Holden, D. J. Robbins, and W. J. Stewart, IEEE Trans. Microwave Theory Tech. **47**, 2075 (1999).
[2] D. R. Smith, W. J. Padilla, D. C. Vier, S. C. Nemat-Nasser, and S. Schultz, Phys. Rev. Lett. **84**, 4184 (2000).
[3] R. A. Shelby, D. R. Smith, and S. Schultz, Science **292**, 77 (2001).
[4] D. Schurig, J. J. Mock, B. J. Justice, S. A. Cummer, J. B. Pendry, A. F. Starr, and D. R. Smith, Science **314**, 977 (2006).
[5] T. Driscoll, Hyun-Tak Kim, Byung-Gyu Chae, Bong-Jun Kim, Yong-Wook Lee, N. Marie Jokerst, S. Palit, D. R. Smith, M. Di Ventra, and D. N. Basov, Science **325**, 1518 (2009).
[6] H. Tao, E. A. Kadlec, A. C. Strikwerda, K. Fan, W. J. Padilla, R. D. Averitt, E. A. Shaner, and X. Zhang, Opt. Express **19**, 21620 (2011).
[7] N. I. Landy, S. Sajuyigbe, J. J. Mock, D. R. Smith, and W. J. Padilla, Phys. Rev. Lett. **100**, 207402 (2008).
[8] H. Tao, C. M. Bingham, A. C. Strikwerda, D. Pilon, D. Shrekenhamer, N. I. Landy, K. Fan, X. Zhang, W. J. Padilla, and R. D. Averitt, Phys. Rev. B **78**, 241103 (2008).
[9] W. J. Padilla, M. T. Aronsson, C. Highstrete, M. Lee, A. J. Taylor, and R. D. Averitt, Phys. Rev. B **75**, 041102 (2007).
[10] S. Hussain, J. M. Woo, and J.-H. Jang, Appl. Phys. Lett. **101**, 091103 (2012).
[11] M. Decker, R. Zhao, C. M. Soukoulis, S. Linden, and M. Wegener, Opt. Lett. **35**, 1593 (2010).
[12] I. B. Vendik, O. G. Vendik, M. A. Odit, D. V. Kholodnyak, S. P. Zubko, M. F. Sitnikova, P. A. Turalchuk, K. N. Zemlyakov, I. V. Munina, D. S. Kozlov, V. M. Turgaliev, A. B. Ustinov, Yeonsang Park, Jinyun Kihm, and Chang-Won Lee, IEEE Transactions on Terahertz Science and Technology **2**, 538 (2012).
[13] M. Lapine, D. Powell, M. Gorkunov, I. Shadrivov, R. Marques, and Y. Kivshar, Appl. Phys. Lett. **95**, 084105 (2009).
[14] Y. H. Fu, A. Q. Liu, W. M. Zhu, X. M. Zhang, D. P. Tsai, J. B. Zhang, T. Mei, J. F. Tao, H. C. Guo, X. H. Zhang, J. H. Teng, N. I. Zheludev, G. Q. Lo, and D. L. Kwong, Adv. Funct. Mater. **21**, 3589 (2011).
[15] M. Lapine, I. V. Shadrivov, D. A. Powell, and Y. S. Kivshar, Nature Materials **11**, 30 (2011).
[16] R. Marques, F. Mesa, J. Martel, and F. Medina, IEEE Trans. Antennas Propag. **51**, 2572 (2003).
[17] E. Ekmekci, A. C. Strikwerda, K. Fan, G. Keiser, X. Zhang, G. Turhan-Sayan, and R. D. Averitt, Phys. Rev. B **83**, 193103 (2011).
[18] R. Marqués, F. Medina, and R. Rafii-El-Idrissi, Phys. Rev. B **65**, 144440 (2002).
[19] D. A. Powell, M. Lapine, M. V. Gorkunov, I. V. Shadrivov, and Y. S. Kivshar, Phys. Rev. B **82**, 155128 (2010).
[20] D. A. Powell, K. Hannam, I. V. Shadrivov, and Y. S. Kivshar, Phys. Rev. B **83**, 235420 (2011).
[21] D. A. Powell and Y. S. Kivshar, Appl. Phys. Lett. **97**, 091106 (2010).
[22] J. Wang, S. Qu, J. Zhang, H. Ma, Y. Yang, C. Gu, X. Wu, and Z. Xu, Prog. Electromagn. Res. Lett. **6**, 35 (2009).
[23] H. A. Haus and W. Huang, Proc. IEEE **79**, 1505 (1991).
[24] N. Liu and H. Giessen, Angew. Chem., Int. Ed. **49**, 9838 (2010).
[25] N. Liu, H. Liu, S. Zhu, and H. Giessen, Nat. Photon. **3**, 157 (2009).